The E3 ubiquitin ligase WWP2 facilitates RUNX2 protein transactivation in a mono-ubiquitination manner during osteogenic differentiation

Received for publication, December 13, 2016, and in revised form, April 29, 2017 Published, Papers in Press, May 12, 2017, DOI 10.1074/jbc.M116.772277

Wei Zhu[1], **Xinyu He**[1], **Yue Hua, Qian Li, Jiyong Wang**[2], **and Xiaoqing Gan**[3]

From the Key Laboratory of Metabolism and Molecular Medicine, Ministry of Education, Department of Biochemistry and Molecular Biology, School of Basic Medical Sciences, Fudan University, Shanghai 200032, China

Edited by George N. DeMartino

Poly-ubiquitination-mediated RUNX2 degradation is an important cause of age- and inflammation-related bone loss. NEDD4 family E3 ubiquitin protein ligases are thought to be the major regulators of RUNX2 poly-ubiquitination. However, we observed a mono-ubiquitination of RUNX2 that was catalyzed by WWP2, a member of the NEDD4 family of E3 ubiquitin ligases. WWP2 has been reported to catalyze the mono-ubiquitination of Goosecoid in chondrocytes, facilitating craniofacial skeleton development. In this study, we found that osteogenic differentiation of mesenchymal stem cells promoted WWP2 expression and nuclear accumulation. Knockdown of *Wwp2* in mesenchymal stem cells and osteoblasts led to significant deficiencies of osteogenesis, including decreased mineral deposition and down-regulation of osteogenic marker genes. Co-immunoprecipitation experiments showed the interaction of WWP2 with RUNX2 *in vitro* and *in vivo*. Mono-ubiquitination by WWP2 leads to RUNX2 transactivation, as evidenced by the wild type of WWP2, but not its ubiquitin ligase-dead mutant, augmenting RUNX2-reponsive reporter activity. Moreover, deletion of WWP2-dependent mono-ubiquitination resulted in striking defects of RUNX2 osteoblastic activity. In addition, ectopic expression of the constitutively active type 1A bone morphogenetic protein receptor enhanced WWP2-dependent RUNX2 ubiquitination and transactivation, demonstrating a regulatory role of bone morphogenetic protein signaling in the WWP2-RUNX2 axis. Taken together, our results provide evidence that WWP2 serves as a positive regulator of osteogenesis by augmenting RUNX2 transactivation in a non-proteolytic mono-ubiquitination manner.

This work was sponsored by National Natural Science Foundation of China Grants 31471317 and 31671466 and Shanghai Pujiang Program Grant 14PJ1400600. The authors declare that they have no conflicts of interest with the contents of this article.

This article contains supplemental Table S1.

[1] Both authors contributed equally to this work.

[2] To whom correspondence may be addressed: Key Laboratory of Metabolism and Molecular Medicine, Ministry of Education, Dept. of Biochemistry and Molecular Biology, School of Basic Medical Sciences, Fudan University, P. O. Box 240, Shanghai 200032, China. Tel.: 86-21-54237661; E-mail: jiyongwang73@gmail.com.

[3] To whom correspondence may be addressed: Key Laboratory of Metabolism and Molecular Medicine, Ministry of Education, Dept. of Biochemistry and Molecular Biology, School of Basic Medical Sciences, Fudan University, P. O. Box 240, Shanghai 200032, China. Tel.: 86-21-54237661; E-mail: xiaoqinggan@fudan.edu.cn.

The maintenance, repair, and remodeling of the skeleton is regulated by constant resorption and formation of bone mineral. Hematopoietically derived osteoclasts control bone resorption, whereas mesenchyme-derived osteoblasts facilitate bone mineral deposition (1). Imbalance of these two processes causes osteoporosis, an age-related skeletal disorder. Among various pathogenic factors associated with osteoporosis, the defect of mesenchyme osteoblast-driven osteogenesis is a significant risk (2, 3).

The transcription factor RUNX2 belongs to the Runt domain-containing gene family, which is a master regulator for osteoblast differentiation as well as for chondrocyte maturation during skeletal development (4, 5). The commitment of mesenchymal progenitors to the osteoblastic lineage requires sequential actions of RUNX2 and the RUNX2 target OSTERIX (6). Targeted disruption of the *Runx2* gene in mice resulted in complete lack of osteoblasts (7, 8). Structurally, RUNX2 proteins possess two functional regions. The N-terminal region is characterized by a highly conserved 128-amino acid region termed the "Runt domain," which is responsible for DNA binding and heterodimerization with the co-factor CBFB (9). The C-terminal region is rich in proline, serine, and threonine, being involved in functional interactions with various other transcriptional coactivators and corepressors (5).

RUNX2 proteins by themselves are often weak transcriptional regulators. On one hand, numerous nuclear factors have been shown to synergize with RUNX2 to promote osteoblast differentiation, such as TAZ, RB, and SATB2, by enhancing RUNX2 activity or acting as co-activators (10–12). Moreover, RUNX2 regulation of target gene expression seems to be modulated by chromatin modifiers in the nucleus (13–15). On the other hand, highly dynamic protein posttranslational modifications, especially protein ubiquitination, play a critical role in RUNX2 activation and bone homeostasis (16–21). A growing body of evidence demonstrates that NEDD4 family HECT-type E3 ubiquitin protein ligases functionally act on osteoblasts and their precursors by degrading a range of key regulators of bone anabolism. NEDD4 family ligases consist of nine members: NEDD4/4L, WWP1/2, ITCH, SMURF1/2, and NEDL1/2. SMURF1 targets MEKK2 degradation and down-regulates bone mass in an age-dependent manner (17, 18). *Wwp1* knockout mice develop increased bone mass as they age, associated with up-regulated protein levels of RUNX2, JUNB, and CXCR-4 (20). TNFα facilitates inflammatory bone loss and

destruction of RUNX2 by up-regulation of SMURF1 and SMURF2 in osteoblasts (21). Although a number of biochemistry data suggest that RUNX2 may be a target of HECT family E3 ligases, the physiological role and molecular mechanism of RUNX2 ubiquitination in osteoblast commitment and differentiation remain controversial. For instance, RUNX2 in *Smurf1*$^{-/-}$ mice does not exhibit significant up-regulation of protein stability (17). Similarly, aged *Wwp1*$^{-/-}$ mice have increased protein stability of JUNB rather than RUNX2 (20).

Recently, Zou *et al.* (22) demonstrated that targeted disruption of *Wwp2* in mice led to profound craniofacial malformation and a shortened trunk because of deficiencies of SOX9-Goosecoid signaling in chondrocytes . In this study, we found that WWP2 might also be involved in the osteogenic differentiation of mesenchymal stem cells and primary osteoblasts. Moreover, WWP2 catalyzes the mono-ubiquitination, but not poly-ubiquitination, of RUNX2, by which WWP2 potentiates the transcriptional and osteoblastic activity of RUNX2. In addition, we identified three lysine residues (Lys-202, Lys-225, and Lys-240) derived from murine Runx2 proteins that are essential for RUNX2 mono-ubiquitination and transactivation. Importantly, missense mutations of Lys-225 and Lys-240 had been identified in human cleidocranial dysplasia, a severe skeletal disorder caused by insufficiency of RUNX2 transcriptional activity (23, 24). Therefore, our results support a positive relevance of WWP2-mediated RUNX2 ubiquitination in RUNX2 activity and skeleton development.

Results

The HECT domain facilitates cytoplasmic retention of WWP2

Western blotting and quantitative PCR assays revealed that the NEDD4 family E3 ubiquitin protein ligase WWP2 was ubiquitously expressed in a variety of tissues, including the skull (Fig. 1, *A* and *B*). We also found that skulls from aged mice exhibited down-regulation of the osteoblast-specific genes *Runx2*, *Bglap*, and *Ptprv* as well as *Wwp2* (Fig. 1*C*). WWP2 has been reported to catalyze poly-ubiquitination of POU5F1 in human embryonic stem cells (25) and mono-ubiquitination of Goosecoid in chondrocytes (22). However, the regulation of WWP2 in mesenchyme-osteoblast transition and osteoblast differentiation remains unclear. Utilizing an *in vitro* C3H10T1/2 cell differentiation model, we examined the expression and the subcellular localization of WWP2 in pre- and post-osteogenic cells. As shown in Fig. 1*D*, a moderate increase in WWP2 expression in post-osteogenic cells was observed. More importantly, the subcellular localization of WWP2 in mesenchymal stem cells was changed during osteogenic differentiation. Immunofluorescence against WWP2 revealed a more evident nuclear localization of WWP2 proteins in post-osteogenic cells (Fig. 1*E*).

WWP2 proteins consist of several modular units, an N-terminal C2 domain, four central WW domains, and a C-terminal catalytic HECT domain. In addition, a non-conserved region of ~200 amino acids is located between the C2 and WW domains. A previous report demonstrated that SOX9 could interact with the N terminus of WWP2 and then recruit WWP2 into the nucleus (26). To illustrate the role of each unit in the regulation of WWP2 nuclear translocation, various HA-tagged truncated mutants of WWP2 proteins were introduced into HEK293T cells, and then immunofluorescences against an HA tag were carried out. The full-length WWP2 and the truncated WWP2 lacking the C2 domain, non-conserved region, or WW domain exhibited similar cytoplasmic localization, but the lack of a catalytic HECT domain resulted in significant nuclear accumulation of WWP2 proteins (Fig. 1, *F* and *G*). This result suggests that WWP2 proteins by themselves can be actively transported into the nucleus in the absence of the HECT domain. Accordingly, we hypothesized that the existence of the HECT domain may block the nuclear localization signal (NLS)[4] of WWP2 proteins or that the HECT domain harbors a strong nuclear export signal (NES).

The NLS is responsible for active transport of nuclear proteins, which is typically characterized by positively charged amino acid clusters (27, 28). However, such a typical NLS is not included in WWP2 proteins. To further verify active nuclear transport of WWP2 proteins, we constructed a mutated RAN GTPase with low GTP-bound capability, RAN^{T24N}. GTP-bound RAN is essential for NLS-dependent nuclear import; thus, expression of RAN^{T24N} in cells can interfere with *in vivo* active nuclear transport processes (29–31). As expected, the nuclear translocation of WWP2-ΔHECT was significantly blocked in RAN^{T24N}-expressing cells (Fig. 1*H*). We also treated cells with leptomycin B (LMB) to block NES-dependent CRM1-mediated nuclear export (32). However, treatment of LMB could not accumulate WWP2 proteins in the nucleus; as a control, NES-facilitated cytoplasmic retention of the nuclear protein GLI was remarkably reversed (Fig. 1*I*). Taken together, the C-terminal HECT domain negatively regulates WWP2 nuclear translocation by suppressing WWP2 active nuclear import rather than enhancing WWP2 nuclear export.

WWP2 positively regulates osteogenesis and RUNX2 transcriptional activity

The commitment of mesenchymal stem cells to osteoblasts and osteoblast differentiation are the main processes of bone anabolism, which declines with aging (33, 34). The expression of WWP2 in bone is negatively correlated with age (Fig. 1*C*). However, WWP2 expression is increased during osteogenic differentiation of mesenchymal stem cells (Fig. 1*D*). Moreover, WWP2 localization is changed to more nuclear retention (Fig. 1*E*). Thus, we speculated that WWP2 may be involved in osteogenic differentiation. To test this idea, we used lentiviruses to transfer *Wwp2*-interfering shRNA into C3H10T1/2 cells. The result, as shown in Fig. 2*A*, was that knockdown of *Wwp2* remarkably reduced the number of mineralized matrix nodules in post-osteogenic cells. Consistent with this, the major osteogenic marker genes *Osterix*, *Alpl*, and *Bglap* were significantly suppressed (Fig. 2*B*). To further demonstrate the osteogenic role of WWP2, we isolated primary osteoblasts from the femur

[4] The abbreviations used are: NLS, nuclear localization signal; NES, nuclear export signal; LMB, leptomycin B; Ni-NTA, nickel-nitrilotriacetic acid; co-IP, co-immunoprecipitation; CCD, cleidocranial dysplasia; BMP, bone morphogenetic protein; CA, constitutively active; qPCR, quantitative real-time PCR; CBFB, core-binding factor subunit β; HECT, homologous to the E6-AP C terminus.

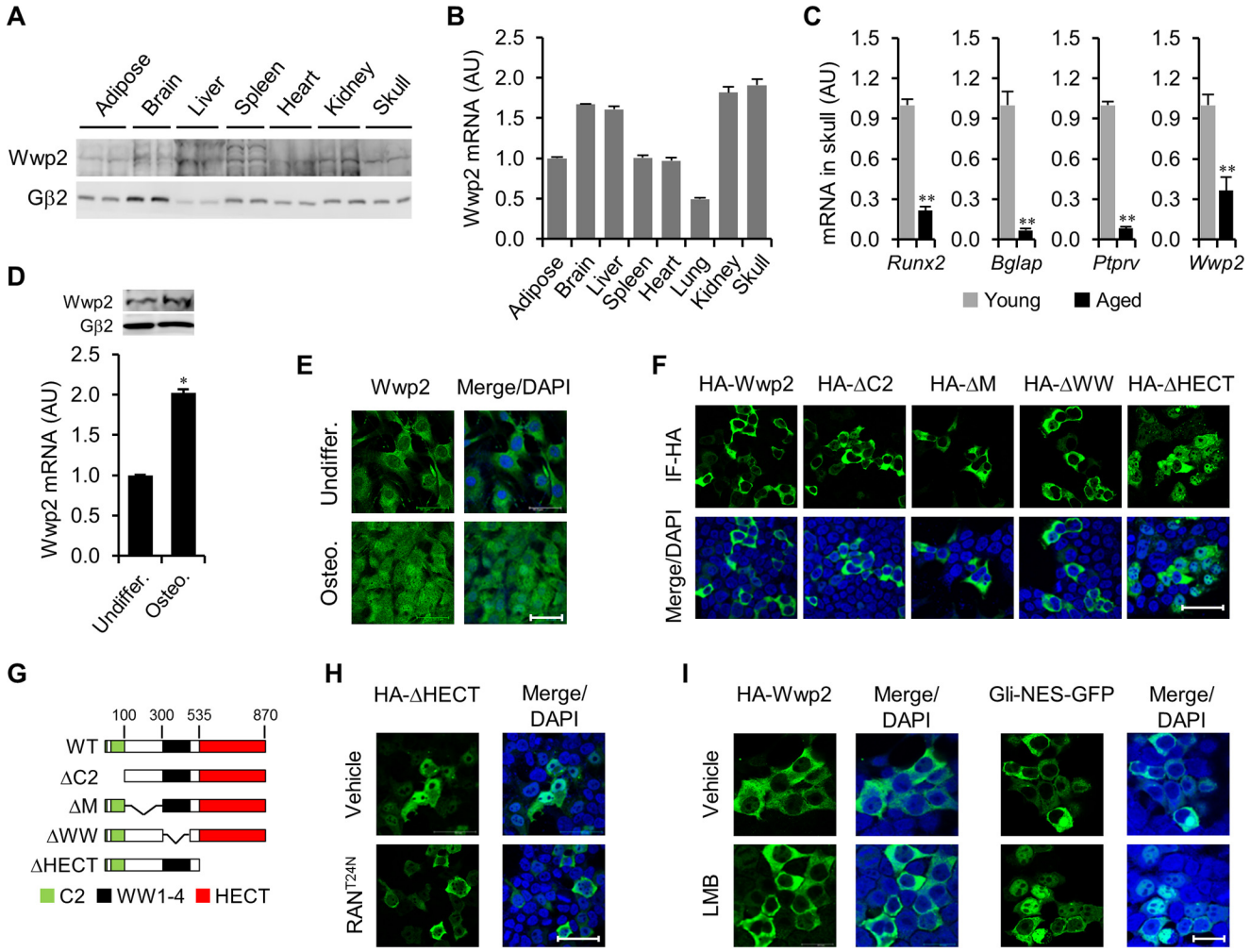

Figure 1. The HECT domain facilitates cytoplasmic retention of WWP2. *A*, examination of WWP2 protein levels in mouse tissues from 8-week-old mice; each sample was a mixture from five mice. *B*, examination of *Wwp2* mRNA levels in mouse tissues from 8-week-old mice ($n = 6$). *AU*, arbitrary unit. *C*, examination of *Wwp2* mRNA levels in skulls from young mice (8 weeks) or aged mice (48 weeks) ($n = 6$). *D*, C3H10T1/2 cells were differentiated into osteocytes as described under "Experimental Procedures." The protein content and mRNA level of *Wwp2* were examined in pre- and post-osteogenic cells. *E*, C3H10T1/2 cells were differentiated into osteocytes (*Osteo*). Immunofluorescence against WWP2 was performed in pre- and post-osteogenic cells. *Scale bar* = 50 μM. *Undiffer*, undifferentiated. *F*, HA-tagged mutants were introduced into HEK293T cells, and immunofluorescence against HA antibody (*IF-HA*) was performed. *Scale bar* = 50 μM. *G*, schematic of truncated mutants of WWP2. *H*, HA-tagged WWP2-ΔHECT was co-expressed with or without RAN^{T24N} in HEK293T cells, and immunofluorescence against HA antibody was performed. *Scale bar* = 50 μM. *I*, HA-tagged WWP2 and NES-fused GLI-GFP were expressed in HEK293T cells overnight, and then cells were treated with LMB (2 μM) for 8 h. Immunofluorescence against HA antibody for WWP2 was performed. *Scale bar* = 50 μM. All data are represented as mean ± S.D. *, $p < 0.05$; **, $p < 0.01$; Student's *t* test; $n = 3$.

of mice. shRNA-mediated inhibition of *Wwp2* expression similarly blocked osteogenic differentiation of osteoblasts (Fig. 2, *C* and *D*). In addition, overexpression of WWP2 in mesenchymal stem cells was capable of enhancing osteogenic marker genes during osteogenesis (Fig. 2, *E* and *F*). Taken together, these results suggest that WWP2 is a positive regulator of osteogenic differentiation.

Expression of the osteogenic markers OSTERIX, BGLAP, and ALPL are transcriptionally controlled by the master transcriptional regulator RUNX2 (6, 14, 35, 36), but we found that alternations of WWP2 expression in osteogenic cells did not affect *Runx2* expression levels (Fig. 2, *B* and *D–F*). At the same time, expressing a truncated Runt domain to compete for DNA occupation with endogenous RUNX2 or decreasing *Runx2* expression by shRNA significantly suppressed WWP2-facilitated expression of osteogenic markers (Fig. 2, *E* and *F*). These results suggest that RUNX2 might function downstream of WWP2 during osteogenic differentiation but that it is not the transcriptional target of WWP2-involved signaling. We then asked how WWP2 regulates RUNX2 actions in osteogenic differentiation. Although WWP2 belongs to the NEDD4 family of E3 ubiquitin protein ligases, overexpression of WWP2 or knockdown of *Wwp2* did not change RUNX2 protein contents (Fig. 3, *A* and *B*). Knockdown of *Wwp2* did not affect the nuclear localization of RUNX2 proteins in osteogenic cells (Fig. 3*C*). These results demonstrate that WWP2 is dispensable to RUNX2 protein stability or subcellular localization in osteogenic cells. Given these findings, we inferred that WWP2 may be involved in the regulation of RUNX2 transcriptional activity.

To examine RUNX2 transcriptional activity *in vitro*, we constructed a luciferase reporter gene containing the Runt DNA-binding consensus sequence 5′-ACCACA-3′. We then performed reporter assays where RUNX2 was co-transfected in

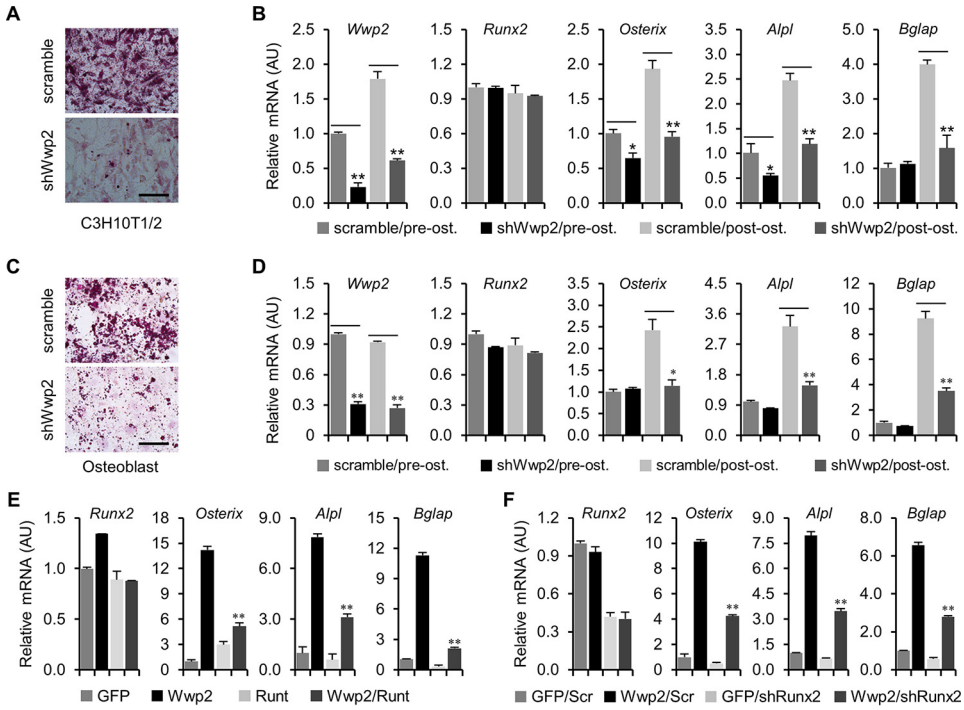

Figure 2. WWP2 positively regulates osteogenesis of C3H10T1/2 cells and primary osteoblasts. *A* and *B*, C3H10T1/2 cells were differentiated into osteocytes in the presence of scrambled or *Wwp2* shRNA. *A*, Alizarin Red S staining on day 21. *Scale bar* = 100 μm. *B*, qPCR for mRNA levels on day 7. *AU*, arbitrary unit. *C* and *D*, osteoblasts from mouse bone marrow were differentiated into osteocytes in the presence of scrambled or *Wwp2* shRNA. *C*, Alizarin Red S staining on day 10. *Scale bar* = 100 μm. *D*, qPCR for mRNA levels on day 4. *E*, C3H10T1/2 cells were infected with lentiviruses as indicated and then differentiated into osteocytes. Runt is constructed from amino acids 108–250 of murine Runx2, including the nuclear localization signal (qPCR for mRNA levels on day 7). *F*, knockdown of Runx2 suppresses WWP2-facilitated expression of osteogenic marker genes. C3H10T1/2 cells were infected with lentiviruses as indicated and then differentiated into osteocytes (qPCR for mRNA levels on day 7). *Scr*, scrambled. All data are represented as mean ± S.D. *, $p < 0.05$; **, $p < 0.01$; Student's *t* test; $n = 3$.

HEK293T cells along with the reporter gene in the absence or presence of WWP2. We observed that RUNX2 alone had faint transcriptional activity, but WWP2 co-expression significantly augmented it (Fig. 3*D*). To further access the regulation of WWP2 in RUNX2 transactivation, we constructed a *Bglap* promoter-based luciferase reporter. Interestingly, we found that RUNX2-facilitated activation of the *Bglap* promoter was remarkably enhanced by WWP2 (Fig. 3*E*). However, thyroid receptor (TRα)-modulated activation was not affected (Fig. 3*E*). Taken together, these results demonstrate that WWP2 can positively regulate RUNX2 transactivation.

The transcriptional activity of RUNX2 is cooperated by its DNA binding domain and transcriptional activation domain. Therefore, we asked which part is regulated by WWP2. The co-factor CBFB has been known to form a heterodimer with RUNX2, thus enhancing RUNX2 DNA binding activity (37, 38). We found that the presence of WWP2 did not increase the affinity of RUNX2 for CBFB (Fig. 3*F*). Moreover, ChIP assays also showed that WWP2 did not affect the association of RUNX2 with reporter DNA (Fig. 3*G*). These results suggest that WWP2 is not involved in regulation of the RUNX2 DNA-binding capacity. Next we pursued whether WWP2 can regulate the transcriptional activation of RUNX2. A fusion of RUNX2 with GAL4-DNA binding domain, DBD-Runx2, was constructed. Using a GAL4-responsive reporter gene, we confirmed that the transcriptional activity of DBD-RUNX2, but not wild-type RUNX2 or the individual GAL4-DBD, was stimulated by the co-expression of WWP2 (Fig. 3*H*). Wild-type RUNX2 cannot recognize and bind to the GAL4-responsive reporter, whereas the individual GAL4-DBD lacks the transcriptional domain. Therefore, this result demonstrates that WWP2 augments the intrinsic transcriptional activation, but not DNA binding capacity, of RUNX2.

WWP2 induces mono-ubiquitination of RUNX2

Osteogenic differentiation induced ubiquitination of RUNX2 proteins that could be eliminated by knockdown of *Wwp2*, suggesting that WWP2 may be involved in RUNX2 ubiquitination modification during osteogenesis of mesenchymal stem cells (Fig. 4*A*). Furthermore, the ubiquitin ligase-dead mutant WWP2-ΔHECT failed to activate RUNX2, whereas the expression of exogenous ubiquitin further enhanced WWP2-stimulated RUNX2 transactivation, demonstrating that the ubiquitin E3 ligase activity of WWP2 is involved in the regulation of RUNX2 transcriptional activity (Fig. 4*B*). To further assess RUNX2 ubiquitination induced by WWP2, we co-expressed RUNX2 along with His-ubiquitin in HEK293T cells. The ubiquitin-conjugated RUNX2 proteins were pulled down by an Ni-NTA column. Western blotting showed that WWP2-co-expression obviously induced RUNX2 ubiquitination (Fig. 4*C*). WWP2 can facilitate both poly-ubiquitination and mono-ubiquitination (22, 25, 39). Because mono-ubiquitination generally causes more activation rather than degradation of target proteins, we next validated whether RUNX2 is mono-ubiquitinated by WWP2. Ub-K0, a mutated ubiquitin in which all seven lysine residues are substituted with arginine residues, can pre-

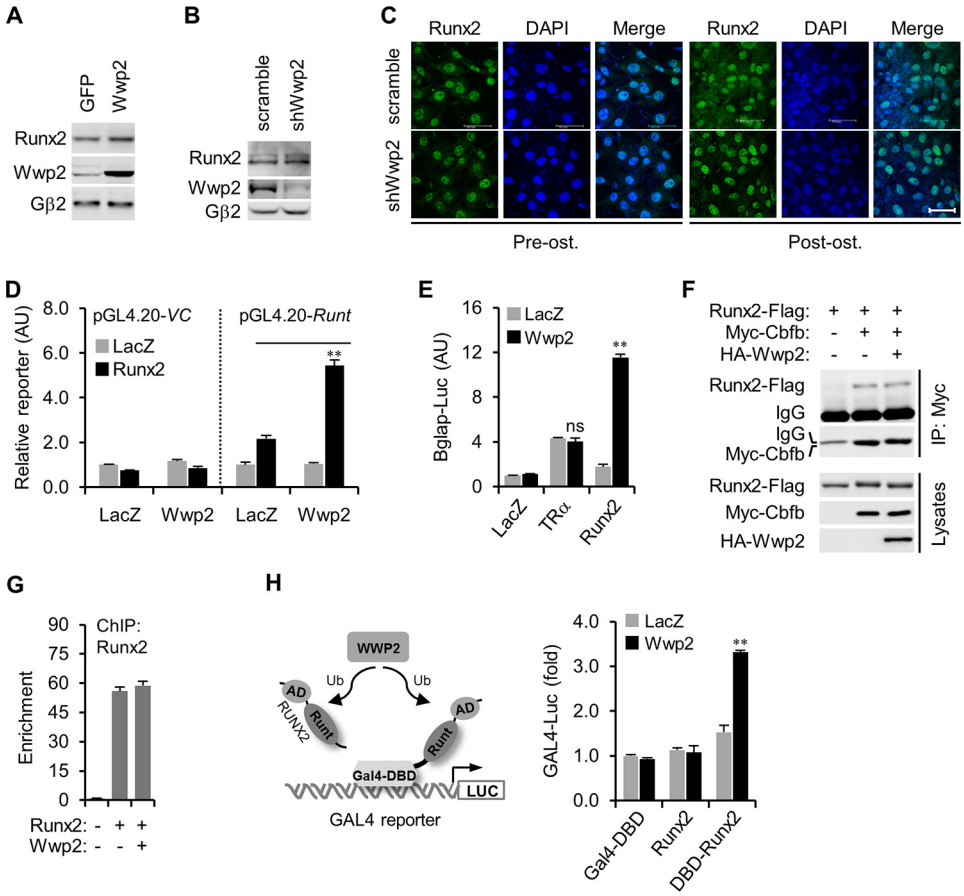

Figure 3. WWP2 activates RUNX2 transcriptional activity. *A*, overexpression of WWP2 in osteogenic C3H10T1/2 cells cannot affect RUNX2 protein content. *B*, knockdown of *Wwp2* in osteogenic C3H10T1/2 cells cannot affect RUNX2 protein content. *C*, knockdown of *Wwp2* cannot affect RUNX2 nuclear localization. *Scale bar* = 50 μM. *Pre-ost*, pre-osteogenesis; *Post-ost*, post-osteogenesis. *D*, Runx2 was co-transfected with vehicle pGL4.20 (pGL4.20-VC) or Runx2-responsive luciferase reporter (pGL4.20-Runt) into HEK293T cells in the absence or presence of WWP2. After 24 h, luciferase reporter assays were performed. *AU*, arbitrary unit. *E*, WWP2 regulates the promoter activity of the *Bglap* gene dependent on RUNX2. Bglap-Luc was constructed by inserting the −1.3-kb promoter of the mouse Bglap gene into the pGL4.20 vector. *F*, the interaction of Myc-Cbfb with Runx2-FLAG was examined in empty or Wwp2-expressing HEK293T cells. *G*, ChIP was performed with a Runx2 antibody in HEK293T cells. The Runt reporter was co-expressed along with Runx2 in empty or WWP2-expressing HEK293T cells. The enriched reporter DNA fragment by Runx2 antibody was quantified by real-time PCR. *H*, Runx2 was fused to the GAL4 DNA-binding domain (DBD-Runx2). The individual GAL4-DBD, wild-type Runx2, or DBD-Runx2 was co-transfected along with a GAL4-responsive luciferase reporter in the absence or presence of WWP2. After 24 h, luciferase reporter assays were performed. *Ub*, ubiquitination; *LUC*, luciferase; *AD*, transcriptional activation domain. All data are represented as mean ± S.D. **, $p < 0.01$; *ns*, not significant; Student's *t* test; $n = 3$.

vent the formation of poly-ubiquitin chains. As expected, the ubiquitination pattern of RUNX2 in Ub-K0-expressing cells was similar to that in wild-type ubiquitin-expressing cells (Fig. 4*D*), suggesting a mono-ubiquitination manner for RUNX2 upon WWP2 co-expression. Consistent with this result, WWP2 did not affect the turnover of RUNX2 proteins (Fig. 4*E*). In addition, WWP2 also catalyzed strong ubiquitination of SMAD1 and weak ubiquitination of SMAD4, the important transcription co-regulators of osteogenesis and bone development (Fig. 4*F*). However, overexpression of WWP2 could not stimulate the transcriptional activity of the SMAD1-SMAD4 complex (Fig. 4*G*). Taken together, we concluded that WWP2 utilizes a distinct non-proteolytic mono-ubiquitination manner to fine-tune the transcriptional activity of RUNX2.

HECT-type E3 ubiquitin ligases facilitate the conjugation of ubiquitin by directly interacting with their target proteins (40). Therefore, we performed co-immunoprecipitation (co-IP) to validate whether RUNX2 is associated with WWP2. We overexpressed FLAG-tagged RUNX2 with or without HA-tagged WWP2 in HEK293T cells, and co-IP experiments were performed with HA antibody. The result, as shown in Fig. 4*H*, was that RUNX2 was well detected in WWP2-containing immunoprecipitation complexes. Next we examined the association of RUNX2 with WWP2 *in vivo*. Because WWP2 is translocated into the nucleus upon osteogenic differentiation, the nuclear extracts from post-osteogenic C3H10T1/2 cells were collected and then subjected to immunoprecipitation against a WWP2 antibody. Western blotting clearly showed that RUNX2 was able to associate with WWP2 in the nuclear extracts (Fig. 4*I*). Although the WW domain of WWP2 can recognize and bind to the proline-rich PP*X*Y motif (41, 42), we found that the PP*X*Y motif was dispensable to the association of RUNX2 with WWP2. Co-IP revealed that the Y433A mutation that destroys the PP*X*Y motif of murine Runx2 could not disrupt the association of RUNX2 with WWP2 (Fig. 4*J*). Moreover, WW domain-deleted WWP2 could bind to RUNX2 proteins as the wild type of WWP2 (data not shown). Consistent with these interaction assays, the transcriptional activity of the Y433A mutant was also able to be stimulated by WWP2 (Fig. 4*K*).

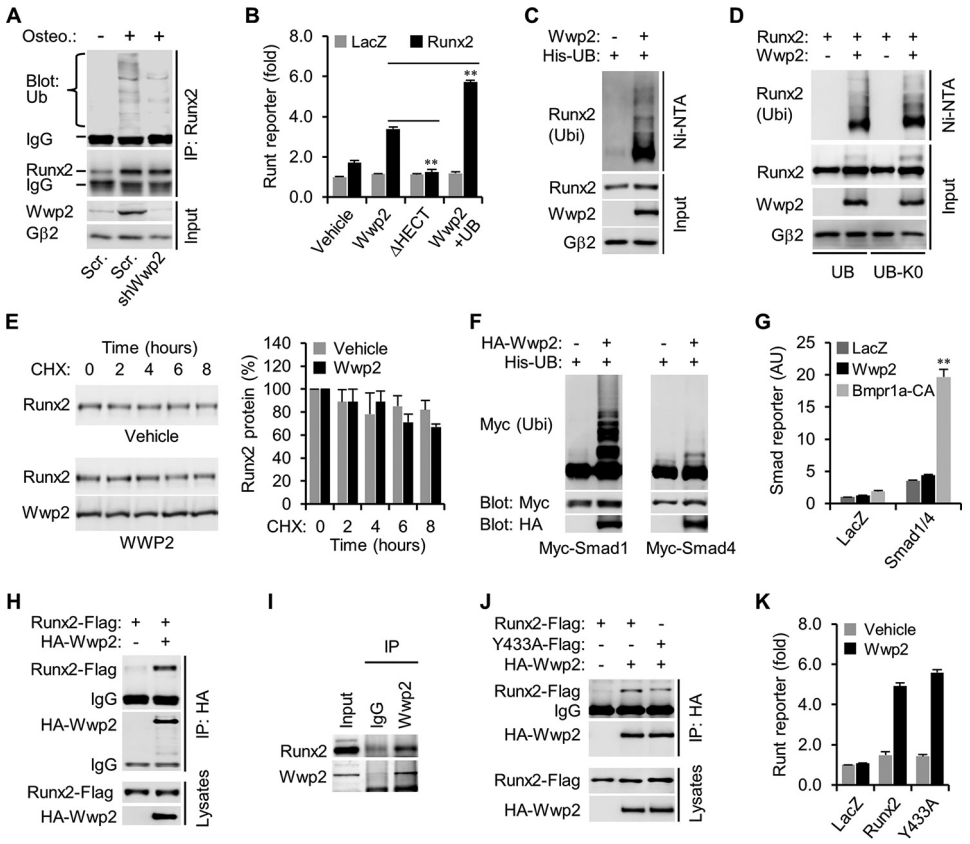

Figure 4. WWP2 induces mono-ubiquitination of RUNX2. *A*, C3H10T1/2 cells were induced by vehicle medium or osteogenic medium in the absence or presence of *Wwp2* shRNA. On day 4 after induction, cells were harvested and lysed. Runx2 proteins were pulled down by a RUNX2 antibody, and then ubiquitination of Runx2 in immunoprecipitation complexes was examined by Western blotting against an ubiquitin antibody. Each sample was prepared from two 10-cm dishes. *Scr*, scrambled. *Ub*, ubiquitin; *Osteo*, osteogenic induction. *B*, WWP2, but not WWP2-ΔHECT, activated the transcription activity of RUNX2 in HEK293T cells. Exogenous ubiquitin further enhanced the WWP2 effects. *C*, Runx2 was co-transfected in HEK293T cells with the indicated plasmids. Ubiquitin-conjugated Runx2 proteins were purified by Ni-NTA column and examined by Western blotting. *D*, WWP2 induced the mono-ubiquitination of Runx2. Runx2 was co-transfected along with His-UB or His-UB-K0, respectively. *E*, the turnover curve of Runx2 protein was examined in empty or WWP2-expressed HEK293T cells. Cells were transfected for 24 h and then treated with cycloheximide (*CHX*, 10 μg/ml) for the indicated times. *Left panel*, Western blotting. *Right panel*, normalized quantification of immunoblots from three independent experiments. *F*, WWP2 induces ubiquitination of Smad1 and Smad4. *G*, WWP2 does not stimulate transcriptional activity of the Smad1-Smad4 complex. Bmp1a-CA was used as a positive control. *AU*, arbitrary unit. *H*, co-immunoprecipitation of FLAG-tagged Runx2 with HA-tagged WWP2 in HEK293T cells. *I*, C3H10T1/2 cells were differentiated into osteocytes. On day 4, the nuclear extracts were subjected to co-immunoprecipitation with a WWP2 antibody. *J*, co-immunoprecipitation of FLAG-tagged Runx2 or Runx2-Y433A with HA-tagged WWP2 in HEK293T cells. *K*, WWP2 stimulates Runx2 or Runx2-Y433A transcriptional activity in HEK293T cells. All data are represented as mean ± S.D. **, $p < 0.01$; Student's *t* test; $n = 3$.

Residues Lys-202, Lys-225, and Lys-240 are essential for RUNX2 ubiquitination

Individual Lys-to-Arg substitutions for all lysine residues were generated in murine Runx2 proteins. We identified three substitutions for Lys-202, Lys-225, and Lys-240 that apparently impaired WWP2-mediated RUNX2 transactivation (Fig. 5*A*). In addition, we observed that the double mutation of Lys-202 and Lys-225 (K2R) resulted in more significant inhibition than the other two double mutations (Fig. 5*B*). The ubiquitination assay also confirmed that the K2R mutation could suppress WWP2-mediated RUNX2 ubiquitination (Fig. 5*C*). In addition, the histone acetyltransferase p300 can induce the acetylation of lysine residues of RUNX2 proteins, thereby stimulating RUNX2 transactivation (15). However, we found that the K2R mutation barely influenced p300-stimulated RUNX2 transcriptional activity (Fig. 5*D*), indicating a dominant role of Lys-202 and Lys-225 for WWP2. Then we investigated the physiological role of WWP2-mediated RUNX2 ubiquitination *in vivo*. C3H10T1/2 cells were introduced with the wild-type or K2R of RUNX2, which then underwent osteogenesis. Immunofluorescence showed that the wild-type and K2R of RUNX2 were expressed in the nuclei of C3H10T/2 cells equally well (Fig. 5*E*). However, K2R-stimulated expression of osteogenic genes and mineralized matrix deposition were significantly lower than those of wild-type RUNX2 (Fig. 5*F*). Interestingly, missense mutations in these lysine residues have been found in patients with cleidocranial dysplasia (CCD), a severe skeletal disease caused by insufficiency of RUNX2 transcriptional activity (23, 24). Thus, we demonstrate that WWP2-modulated RUNX2 ubiquitination may play an important role in osteogenesis and skeleton development.

The type 1A BMP receptor potentiates the WWP2-RUNX2 axis

RUNX2 is a major target of BMP signaling at the transcriptional level (43). Furthermore, BMP signaling has also been reported to regulate RUNX2 posttranslational modification. For instance, BMP-2 can stimulate the acetylation of RUNX2 at residues Lys-240, Lys-245, Lys-365, and Lys-366 via the histone

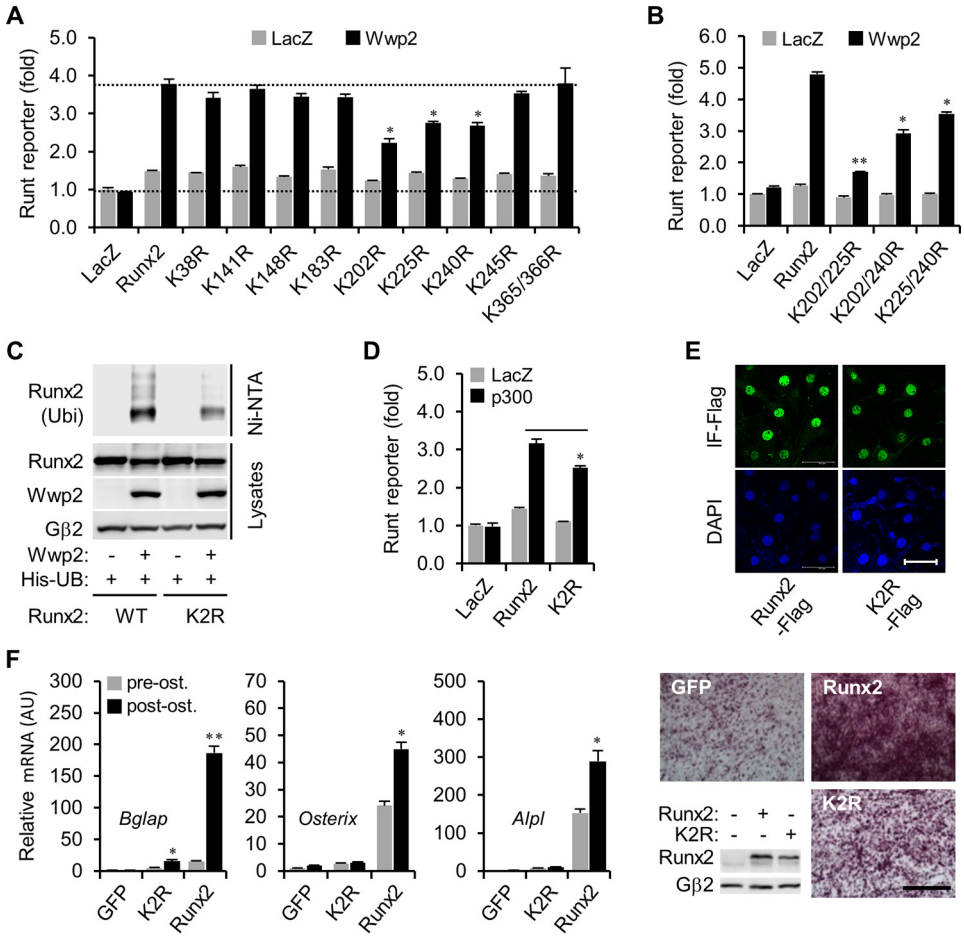

Figure 5. Residues Lys-202, Lys-225, and Lys-240 are essential for RUNX2 ubiquitination. *A*, individual KR substitutions of murine Runx2 proteins in reporter assays with or without WWP2 in HEK293T cells. *B*, the double mutations K202R/K225R, K202R/K240R, and K225R/K240R impaired WWP2-stimulated RUNX2 transactivation in HEK293T cells. *C*, the K2R mutation decreased WWP2-catalyzed ubiquitination (*Ubi*) of RUNX2. *D*, the K2R mutation weakly inhibits p300-mediated RUNX2 transactivation. *E*, immunofluorescence (*IF*) of FLAG-tagged Runx2 and Runx2-K2R in C3H10T1/2 cells. *Scale bar* = 50 μm. *F*, C3H10T1/2 cells were infected with lentiviruses expressing GFP, Runx2-FLAG, or K2R-FLAG and then differentiated into osteocytes. qPCR was performed on day 7 and Alizarin Red S staining on day 21. *Scale bar* = 100 μm. The Western blot shows the expression of Runx2 and Runx2-FLAG in post-osteogenic cells. All data are represented as mean ± S.D. *, $p < 0.05$; **, $p < 0.01$; Student's *t* test; $n = 3$.

acetyltransferase p300 (15). We then asked whether BMP signaling is also involved in WWP2-modulated RUNX2 ubiquitination. The constitutively active form of the type 1A BMP receptor, Bmpr1a-CA, was expressed in HEK293T cells to mimic the activation of BMP signaling (44). Indeed, co-expression of Bmpr1a-CA obviously enhanced WWP2-modulated RUNX2 ubiquitination (Fig. 6*A*). Consistent with the ubiquitination assay, WWP2-dependent RUNX2 transcriptional activity was also augmented by Bmpr1a-CA (Fig. 6*B*). Interestingly, the K2R mutation of RUNX2 completely suppressed this regulation. In addition, overexpression of regulatory SMAD1 could not promote RUNX2 ubiquitination (Fig. 6*C*), indicating that BMP signaling activates the WWP2-RUNX2 axis independent of the regulatory SMAD. To further access the mechanism employed by Bmpr1a-CA, we examined whether Bmpr1a-CA regulates the interaction of WWP2 with RUNX2. The result, as shown in Fig. 6*D*, was that the association of WWP2 with RUNX2 was significantly enhanced by overexpression of Bmpr1a-CA. Unexpectedly, we also observed an obvious protein interaction between WWP2 and the intracellular domain of Bmpr1a-CA (Fig. 6*E*). Taken together, our results suggest that BMP signaling can modulate RUNX2 ubiquitination by enhancing the association of RUNX2 with WWP2, and this regulation is likely to involve the interaction between WWP2 and the BMP receptor.

Discussion

The transcriptional activity of the Runt domain-containing nuclear factor RUNX2 is indispensable for osteoblast differentiation during both intramembranous and endochondral ossification (4–8). Depending on the time and location during the differentiation of osteoblasts and chondrocytes, RUNX2 is transcriptionally activated by various extracellular signals; for instance, BMPs, FGFs, and retinoic acid (4). Numerous nuclear co-activators and co-repressors, such as CBFB, TAZ, RB, and TLE, also temporally fine-tune the transcriptional stiffness of RUNX2 proteins (10, 11, 37, 38, 45). Here we demonstrated a novel mono-ubiquitination-dependent RUNX2 transactivation to modulate the osteogenic differentiation of mesenchymal stem cells.

NEDD4 family E3 ubiquitin protein ligases such as SMURF1/2 and WWP1 are implicated in age-related bone loss and promote the degradation of a range of key regulators of bone anabolism, including components of the MEKK2-JNK-

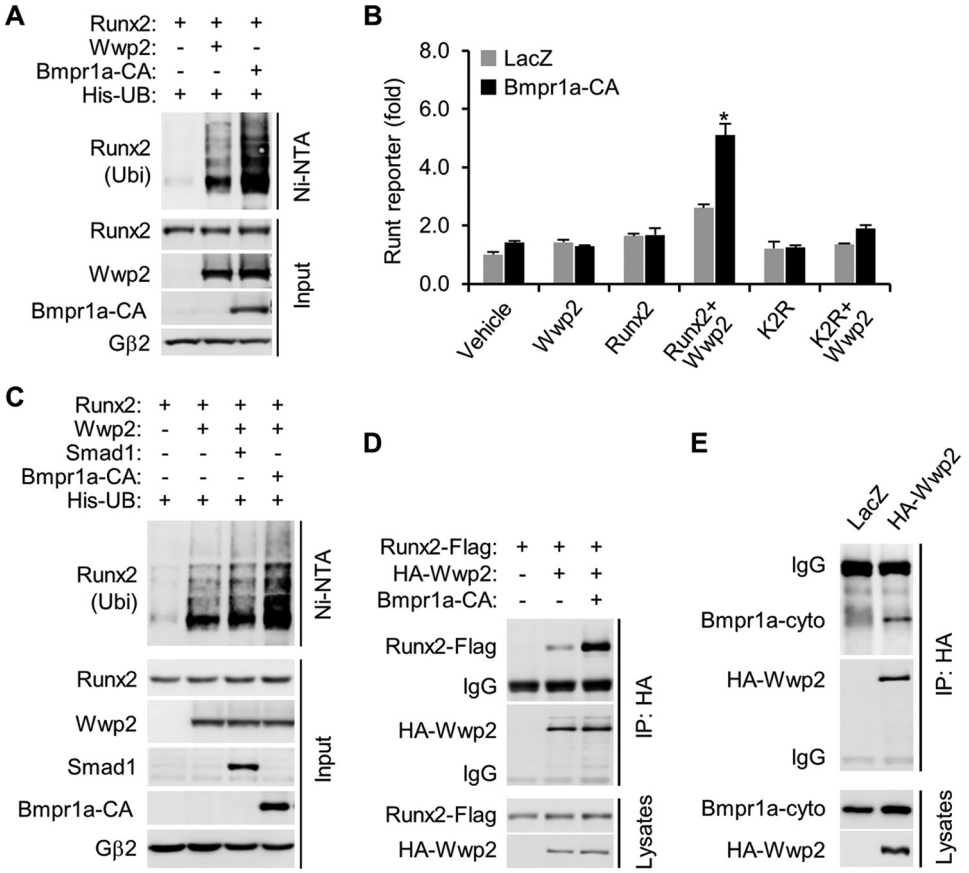

Figure 6. The type 1A BMP receptor potentiates the WWP2-RUNX2 axis. *A*, Bmpr1a-CA enhanced WWP2-dependent RUNX2 ubiquitination. *UB*, ubiquitin; *Ubi*, ubiquitination. *B*, Bmpr1a-CA augmented WWP2-dependent RUNX2 transactivation. *C*, Smad1 is dispensable for WWP2-dependent RUNX2 ubiquitination. *D*, Bmpr1a-CA enhanced the interaction of WWP2 with RUNX2. *E*, co-immunoprecipitation of the cytoplasmic domain of Bmpr1a-CA interacting with HA-tagged WWP2 in HEK293T cells. All data are represented as mean ± S.D. *, $p < 0.05$; Student's *t* test; $n = 3$.

JUNB cascade and the bone master regulator RUNX2 (17–21). However, the member of NEDD4 family E3 ubiquitin ligases WWP2 has been demonstrated to positively regulate skeleton development by activating the SOX9 signaling cascade in chondrocytes (22, 26). In this study, we observed an age-related decline of WWP2 expression in bone tissues. Moreover, osteogenic differentiation of mesenchymal stem cells promotes not only the expression but also the nuclear accumulation of WWP2. Given these results, we hypothesized that WWP2 might be involved in osteogenesis of mesenchymal stem cells. Indeed, knockdown of *Wwp2* in either C3H10T1/2 cells or primary osteoblasts remarkably suppressed main osteogenic genes and bone mineral deposition in post-osteogenic cells. Interestingly, we found that alternations of WWP2 expression in post-osteogenic cells could significantly influence the transcriptional levels of RUNX2-controlled targets, whereas the transcription level, protein stability, and nuclear localization of RUNX2 itself were all unaffected. Accordingly, we speculated that WWP2 could regulate the transcriptional activity of RUNX2. Using a RUNX2-responsive reporter gene, we verified that WWP2 did promote the transcriptional activity of RUNX2. Further studies showed that WWP2 could not regulate the DNA-binding capacity but, rather, regulated the activity of the transcriptional activation domain of RUNX2.

WWP2 modulates the ubiquitination of RUNX2 during osteogenesis, suggesting the involvement of WWP2 in RUNX2 ubiquitination. E3 ligase-dead WWP2 failed to activate RUNX2, whereas expression of exogenous ubiquitin in cells could further enhance WWP2-stimulated RUNX2 transcriptional activity, demonstrating that the E3 ligase activity of WWP2 is essential for RUNX2 transactivation. Protein interaction and ubiquitination assays confirmed that WWP2 can bind to RUNX2 *in vitro* and *in vivo* and catalyze the ubiquitination of RUNX2. Importantly, WWP2 catalyzes RUNX2 in a non-proteolytic, mono-ubiquitination manner. This result was consistent with the observation that WWP2 could not accelerate the turnover of RUNX2 proteins. In addition, we provide evidence to demonstrate that BMP signaling may participate in the regulation of the WWP2-RUNX2 axis. The constitutively active BMPR1A can promote WWP2-dependent RUNX2 ubiquitination and transactivation by enhancing the association of RUNX2 and WWP2. The association of WWP2 with the intracellular domain of BMPR1A further supports the involvement of BMP signaling in the WWP2-RUNX2 axis.

Finally, the analyses of individual KR mutations revealed that residues Lys-202, Lys-225, and Lys-240 are essential for WWP2-mediated RUNX2 ubiquitination and activation. The double mutation K202R/K225R (K2R) had the most inhibitory effect on WWP2-dependent RUNX2 activation, whereas further mutation of K240R (K202R/K225R/K240R) did not enhance K2R inhibition (data not shown), suggesting that Lys-202 appears to be the most essential amino acid residue in

WWP2-dependent RUNX2 transactivation. The physiological role of WWP2-modulated RUNX2 ubiquitination was validated by overexpressing the K2R mutant in post-osteogenic C3H10T1/2 cells. As expected, either osteogenic marker genes or mineral deposition was remarkably inhibited in K2R-expressed cells. Furthermore, analyses of somatic mutations of *RUNX2* gene in human autosomal dominant CCD revealed a number of missense mutations, including K218E, K218Q, and K233R, corresponding to K225E, K225Q, and K240R of the murine *Runx2* gene, respectively (23, 24). The phenotypes of CCD comprise mild dental abnormalities only to severe osteoporosis and clavicular hypoplasia. The insufficiency of RUNX2 transcriptional activity is a major cause of the development of CCD. Therefore, our findings provide insight into how missense mutations affect RUNX2 transcriptional and osteoblastic activity during skeleton development.

Experimental procedures

Antibodies and oligos

Protein A/G-Plus-agarose beads were purchased from Santa Cruz Biotechnology (Santa Cruz, CA). Antibodies to RUNX2 (mAb D1H7, 1:1000, 8486) were purchased from Cell Signaling Technology (Danvers, MA), WWP2 (1:1000, ab103527) from Abcam (Cambridge, UK), Gβ2 (C-16, 1:1000, sc-380) and ubiquitin (1:500, sc-8017) from Santa Cruz Biotechnology, HA.11 (16B12, 1:1000, 901514) and Myc (9E10, 1:1000, 626802) from Biolegend (San Diego, CA), and FLAG M2 (1:1000, F3165) from Sigma-Aldrich (St. Louis, MO). The oligos for gene silencing and real-time PCR used in this study are listed in supplemental Table S1.

Animals

The 4-week-old C57BL/6 mice were from the Shanghai Laboratory Animal Center of the Chinese Academy of Sciences. All experiments were approved by the Animal Care and Use Committee of Fudan University Shanghai Medical College.

Cell culture

HEK293T and C3H10T1/2 cells were maintained in DMEM with 10% FBS and 1× GlutaMAX (Life Technologies) at 37 °C and 5% CO_2. Osteoblasts were isolated from long bones of C57BL/6J mice as described previously (46). Briefly, long bones were harvested and cleaned, and bone marrow was flushed out. Pieces of bone were incubated in collagenase solution at 37 °C, each time for 20 min, repeated four times. Supernatants from the last digestion were collected and cultured in α-minimum Eagle's medium with 10% FBS and 1× GlutaMAX at 37 °C and 5% CO_2.

Reporter assay

HEK293T cells were transiently transfected with DNA using Lipofectamine LTX from Life Technologies according to the instructions of the manufacturer. The LacZ plasmid was added to make the total amount of DNA equal (0.25 μg/well in a 48-well plate). The Runt-responsive luciferase reporter was constructed by inserting the Runt DNA-binding consensus sequence 5′-ACCACA-3′ into the pGL4.20 vector. The Bglap-luciferase reporter was constructed by inserting the −1.3 kb promoter of the mouse *Bglap* gene into the pGL4.20 vector. The Smad-responsive SBE-luciferase reporter was constructed by inserting the 6× Smad-binding consensus sequence 5′-GTCT-3′ into the pGL4.20 vector. The GAL4-reponsive luciferase reporter was constructed by inserting the GAL4 DNA-binding consensus sequence 5′-GGTACTCCAGTCACTCCGCGGATGACGCGACACACCGCGGAAATCCTCACACTCCG-3′ into the pGL4.20 vector. Luciferase reporter assays were performed, and the luciferase activities presented were normalized against the levels of GFP expression as described previously (47).

Viruses

Lentiviruses were constructed with the pLVX-puro vector (Clontech, Mountain View, CA) for gene expression and the pLKO.1 vector (Addgene, Cambridge, MA) for shRNA expression. To prepare viruses, carrier vectors were packaged with the helper plasmids dR8.9 and VSVG and purified by ultracentrifugation. Cells were infected with viruses at a multiplicity of infection of 10.

Gene transcription analysis

Total RNAs were isolated from mouse tissues using a magnetic bead homogenizer in TRIzol reagent or from cultured cells by directly adding TRIzol reagent to the cells. cDNAs were synthesized using the ProtoScript II first strand cDNA synthesis kit (BioLabs, Ipswich, MA). Quantitative real-time PCR (qPCR) analysis was performed using a Power SYBR Green PCR Master Mix (Life Technologies). 18S RNA levels were used as internal controls in the qPCR analysis.

Protein interaction and complex assays

Co-IP experiments were carried out in HEK293T cells. In brief, cells were transfected with the indicated constructs for 24 h and then lysed in a cell lysis buffer (20 mM Tris-HCl (pH 7.5), 150 mM NaCl, 1% Triton X-100, 0.5 mM EDTA, protease inhibitor mixture (Roche), and phosphatase inhibitor mixture (Roche)). After centrifugation, the supernatants were pulled down by the indicated antibodies and then analyzed by immunoblotting. For analysis of endogenous protein complexes in post-osteogenic C3H10T1/2 cells, nuclear extracts from 5×10^7 cells were collected in 1 ml of buffer containing 20 mM Tris-HCl (pH 7.4), 300 mM NaCl, 1% Triton X-100, 2 mM EDTA, protease inhibitor mixture, and phosphatase inhibitor mixture.

Immunofluorescence

Cells on coverslips were washed once with Dulbecco's phosphate-buffered saline (14190136, Invitrogen) and then fixed for 20 min in DPBS containing 4% paraformaldehyde at room temperature. Fixed cells were permeabilized by 0.1% Triton X-100 for 5 min and then blocked by 2% BSA for 30 min. Finally, cells were stained with primary antibodies followed by FITC-conjugated secondary antibodies. Immunofluorescence images were captured using Leica SP5.

Ubiquitination analysis

The indicated constructs were co-transfected into HEK293T cells along with His-ubiquitin for 24 h, and then cells were harvested in a denaturing buffer (6 M guanidine-HCl, 0.1 M Na_2HPO_4/NaH_2PO_4 (pH 8.0), and 10 mM imidazole). The lysates were incubated with Ni-NTA-agarose beads for 3 h, followed by four washes with denaturing buffer and two washes with a low-salt buffer (25 mM Tris-HCl (pH 6.8) and 20 mM imidazole). Ubiquitinated proteins were eluted by boiling in SDS sample buffer in the presence of 200 mM imidazole. After centrifugation, the supernatants were analyzed by immunoblotting (48).

Chromatin immunoprecipitation

ChIP assays in cultured cells were performed as according to the instructions of the manufacturer with a ChIP assay kit (Millipore).

Cell differentiation

Primary osteoblasts were seeded at a density of 4.5×10^5 cells/6-well plate (Corning, 3516) and maintained in α-minimum Eagle's medium (glucose, 5.6 mM). Cells at 80% confluence were induced by osteogenic medium containing 0.1 μM dexamethasone, 0.2 mM ascorbic acid (Sigma), and 10 mM β-glycerophosphate (Sigma) for 7–21 days. For osteogenic differentiation of C3H10T1/2 cells, cells were seeded at a density of 4.5×10^5 cells/6-well plate and maintained in DMEM. Three days after osteogenic induction, the concentration of glucose in DMEM was reduced to 5.6 mM. Quantitative PCR assays were performed on day 7 after osteogenic induction. For Alizarin Red S staining, differentiated cells were fixed with 4% paraformaldehyde for 30 min. Then we removed paraformaldehyde, washed the cells with water twice, and stained them with Alizarin Red S solution for 1 h.

Statistical analysis

We used two-tailed Student *t* tests to evaluate statistical significance and $p < 0.05$ to declare a statistically significant change. We present all values as mean ± S.D.

Author contributions—W. Z. performed the protein ubiquitination and interaction assays. X. H. performed the reporter, cell differentiation, and qPCR assays. Y. H. and Q. L. made the mouse tissue samples and constructs. J. W. supervised the project and wrote the manuscript. X. G. supervised the project and wrote the manuscript.

Acknowledgments—We thank Y. Huang and J. Li for technical help with confocal microscopy.

References

1. Karsenty, G., and Wagner, E. F. (2002) Reaching a genetic and molecular understanding of skeletal development. *Dev. Cell* **2,** 389–406
2. Gibon, E., Lu, L., and Goodman, S. B. (2016) Aging, inflammation, stem cells, and bone healing. *Stem. Cell Res. Ther.* **7,** 44
3. Bidwell, J. P., Alvarez, M. B., Hood, M., Jr., and Childress, P. (2013) Impairment of bone formation in the pathogenesis of osteoporosis: the bone marrow regenerative competence. *Curr. Osteoporos. Rep.* **11,** 117–125
4. Komori, T. (2005) Regulation of skeletal development by the Runx family of transcription factors. *J. Cell. Biochem.* **95,** 445–453
5. Long, F. (2011) Building strong bones: molecular regulation of the osteoblast lineage. *Nat. Rev. Mol. Cell. Biol.* **13,** 27–38
6. Sinha, K. M., and Zhou, X. (2013) Genetic and molecular control of Osterix in skeletal formation. *J. Cell. Biochem.* **114,** 975–984
7. Komori, T., Yagi, H., Nomura, S., Yamaguchi, A., Sasaki, K., Deguchi, K., Shimizu, Y., Bronson, R. T., Gao, Y. H., Inada, M., Sato, M., Okamoto, R., Kitamura, Y., Yoshiki, S., and Kishimoto, T. (1997) Targeted disruption of Cbfa1 results in a complete lack of bone formation owing to maturational arrest of osteoblasts. *Cell* **89,** 755–764
8. Otto, F., Thornell, A. P., Crompton, T., Denzel, A., Gilmour, K. C., Rosewell, I. R., Stamp, G. W., Beddington, R. S., Mundlos, S., Olsen, B. R., Selby, P. B., and Owen, M. J. (1997) Cbfa1, a candidate gene for cleidocranial dysplasia syndrome, is essential for osteoblast differentiation and bone development. *Cell* **89,** 765–771
9. Bäckström, S., Wolf-Watz, M., Grundström, C., Härd, T., Grundström, T., and Sauer, U. H. (2002) The RUNX1 Runt domain at 1.25A resolution: a structural switch and specifically bound chloride ions modulate DNA binding. *J. Mol. Biol.* **322,** 259–272
10. Hong, J. H., Hwang, E. S., McManus, M. T., Amsterdam, A., Tian, Y., Kalmukova, R., Mueller, E., Benjamin, T., Spiegelman, B. M., Sharp, P. A., Hopkins, N., and Yaffe, M. B. (2005) TAZ, a transcriptional modulator of mesenchymal stem cell differentiation. *Science* **309,** 1074–1078
11. Calo, E., Quintero-Estades, J. A., Danielian, P. S., Nedelcu, S., Berman, S. D., and Lees, J. A. (2010) Rb regulates fate choice and lineage commitment *in vivo*. *Nature* **466,** 1110–1114
12. Dobreva, G., Chahrour, M., Dautzenberg, M., Chirivella, L., Kanzler, B., Fariñas, I., Karsenty, G., and Grosschedl, R. (2006) SATB2 is a multifunctional determinant of craniofacial patterning and osteoblast differentiation. *Cell* **125,** 971–986
13. Vega, R. B., Matsuda, K., Oh, J., Barbosa, A. C., Yang, X., Meadows, E., McAnally, J., Pomajzl, C., Shelton, J. M., Richardson, J. A., Karsenty, G., and Olson, E. N. (2004) Histone deacetylase 4 controls chondrocyte hypertrophy during skeletogenesis. *Cell* **119,** 555–566
14. Sierra, J., Villagra, A., Paredes, R., Cruzat, F., Gutierrez, S., Javed, A., Arriagada, G., Olate, J., Imschenetzky, M., Van Wijnen, A. J., Lian, J. B., Stein, G. S., Stein, J. L., and Montecino, M. (2003) Regulation of the bone-specific osteocalcin gene by p300 requires Runx2/Cbfa1 and the vitamin D3 receptor but not p300 intrinsic histone acetyltransferase activity. *Mol. Cell. Biol.* **23,** 3339–3351
15. Jeon, E. J., Lee, K. Y., Choi, N. S., Lee, M. H., Kim, H. N., Jin, Y. H., Ryoo, H. M., Choi, J. Y., Yoshida, M., Nishino, N., Oh, B. C., Lee, K. S., Lee, Y. H., and Bae, S. C. (2006) Bone morphogenetic protein-2 stimulates Runx2 acetylation. *J. Biol. Chem.* **281,** 16502–16511
16. Li, X., Huang, M., Zheng, H., Wang, Y., Ren, F., Shang, Y., Zhai, Y., Irwin, D. M., Shi, Y., Chen, D., and Chang, Z. (2008) CHIP promotes Runx2 degradation and negatively regulates osteoblast differentiation. *J. Cell Biol.* **181,** 959–972
17. Yamashita, M., Ying, S. X., Zhang, G. M., Li, C., Cheng, S. Y., Deng, C. X., and Zhang, Y. E. (2005) Ubiquitin ligase Smurf1 controls osteoblast activity and bone homeostasis by targeting MEKK2 for degradation. *Cell* **121,** 101–113
18. Zhao, L., Huang, J., Guo, R., Wang, Y., Chen, D., and Xing, L. (2010) Smurf1 inhibits mesenchymal stem cell proliferation and differentiation into osteoblasts through JunB degradation. *J. Bone. Miner. Res.* **25,** 1246–1256
19. Zhao, M., Qiao, M., Oyajobi, B. O., Mundy, G. R., and Chen, D. (2003) E3 ubiquitin ligase Smurf1 mediates core-binding factor α1/Runx2 degradation and plays a specific role in osteoblast differentiation. *J. Biol. Chem.* **278,** 27939–27944
20. Shu, L., Zhang, H., Boyce, B. F., and Xing, L. (2013) Ubiquitin E3 ligase Wwp1 negatively regulates osteoblast function by inhibiting osteoblast differentiation and migration. *J. Bone Miner. Res.* **28,** 1925–1935
21. Kaneki, H., Guo, R., Chen, D., Yao, Z., Schwarz, E. M., Zhang, Y. E., Boyce, B. F., and Xing, L. (2006) Tumor necrosis factor promotes Runx2 degradation through up-regulation of Smurf1 and Smurf2 in osteoblasts. *J. Biol. Chem.* **281,** 4326–4333
22. Zou, W., Chen, X., Shim, J. H., Huang, Z., Brady, N., Hu, D., Drapp, R., Sigrist, K., Glimcher, L. H., and Jones, D. (2011) The E3 ubiquitin ligase

Wwp2 regulates craniofacial development through mono-ubiquitylation of Goosecoid. *Nat. Cell Biol.* **13,** 59–65
23. Ott, C. E., Leschik, G., Trotier, F., Brueton, L., Brunner, H. G., Brussel, W., Guillen-Navarro, E., Haase, C., Kohlhase, J., Kotzot, D., Lane, A., Lee-Kirsch, M. A., Morlot, S., Simon, M. E., Steichen-Gersdorf, E., *et al.* (2010) Deletions of the RUNX2 gene are present in about 10% of individuals with cleidocranial dysplasia. *Hum. Mutat.* **31,** E1587–E1593
24. Yoshida, T., Kanegane, H., Osato, M., Yanagida, M., Miyawaki, T., Ito, Y., and Shigesada, K. (2002) Functional analysis of RUNX2 mutations in Japanese patients with cleidocranial dysplasia demonstrates novel genotype-phenotype correlations. *Am. J. Hum. Genet.* **71,** 724–738
25. Xu, H., Wang, W., Li, C., Yu, H., Yang, A., Wang, B., and Jin, Y. (2009) WWP2 promotes degradation of transcription factor OCT4 in human embryonic stem cells. *Cell Res.* **19,** 561–573
26. Nakamura, Y., Yamamoto, K., He, X., Otsuki, B., Kim, Y., Murao, H., Soeda, T., Tsumaki, N., Deng, J. M., Zhang, Z., Behringer, R. R., Crombrugghe, Bd., Postlethwait, J. H., Warman, M. L., Nakamura, T., and Akiyama, H. (2011) Wwp2 is essential for palatogenesis mediated by the interaction between Sox9 and mediator subunit 25. *Nat. Commun.* **2,** 251
27. Lee, B. J., Cansizoglu, A. E., Süel, K. E., Louis, T. H., Zhang, Z., and Chook, Y. M. (2006) Rules for nuclear localization sequence recognition by karyopherin β 2. *Cell* **126,** 543–558
28. Makkerh, J. P., Dingwall, C., and Laskey, R. A. (1996) Comparative mutagenesis of nuclear localization signals reveals the importance of neutral and acidic amino acids. *Curr. Biol.* **6,** 1025–1027
29. Avis, J. M., and Clarke, P. R. (1996) Ran, a GTPase involved in nuclear processes: its regulators and effectors. *J. Cell Sci.* **109,** 2423–2427
30. Cingolani, G., Bednenko, J., Gillespie, M. T., and Gerace, L. (2002) Molecular basis for the recognition of a nonclassical nuclear localization signal by importin β. *Mol. Cell* **10,** 1345–1353
31. Vetter, I. R., Arndt, A., Kutay, U., Görlich, D., and Wittinghofer, A. (1999) Structural view of the Ran-Importin β interaction at 2.3 Å resolution. *Cell* **97,** 635–646
32. Petosa, C., Schoehn, G., Askjaer, P., Bauer, U., Moulin, M., Steuerwald, U., Soler-López, M., Baudin, F., Mattaj, I. W., and Müller, C. W. (2004) Architecture of CRM1/Exportin1 suggests how cooperativity is achieved during formation of a nuclear export complex. *Mol. Cell* **16,** 761–775
33. Krings, A., Rahman, S., Huang, S., Lu, Y., Czernik, P. J., and Lecka-Czernik, B. (2012) Bone marrow fat has brown adipose tissue characteristics, which are attenuated with aging and diabetes. *Bone* **50,** 546–552
34. Bethel, M., Chitteti, B. R., Srour, E. F., and Kacena, M. A. (2013) The changing balance between osteoblastogenesis and adipogenesis in aging and its impact on hematopoiesis. *Curr. Osteoporos. Rep.* **11,** 99–106
35. Paredes, R., Arriagada, G., Cruzat, F., Olate, J., Van Wijnen, A., Lian, J., Stein, G., Stein, J., and Montecino, M. (2004) The Runx2 transcription factor plays a key role in the 1α,25-dihydroxy vitamin D3-dependent upregulation of the rat osteocalcin (OC) gene expression in osteoblastic cells. *J. Steroid Biochem. Mol. Biol.* **89,** 269–271
36. Weng, J. J., and Su, Y. (2013) Nuclear matrix-targeting of the osteogenic factor Runx2 is essential for its recognition and activation of the alkaline phosphatase gene. *Biochim. Biophys. Acta* **1830,** 2839–2852
37. Yoshida, C. A., Furuichi, T., Fujita, T., Fukuyama, R., Kanatani, N., Kobayashi, S., Satake, M., Takada, K., and Komori, T. (2002) Core-binding factor β interacts with Runx2 and is required for skeletal development. *Nat. Genet.* **32,** 633–638
38. Kundu, M., Javed, A., Jeon, J. P., Horner, A., Shum, L., Eckhaus, M., Muenke, M., Lian, J. B., Yang, Y., Nuckolls, G. H., Stein, G. S., and Liu, P. P. (2002) Cbfβ interacts with Runx2 and has a critical role in bone development. *Nat. Genet.* **32,** 639–644
39. Jung, J. G., Stoeck, A., Guan, B., Wu, R. C., Zhu, H., Blackshaw, S., Shih, I. M., and Wang, T. L. (2014) Notch3 interactome analysis identified WWP2 as a negative regulator of Notch3 signaling in ovarian cancer. *PLoS Genet.* **10,** e1004751
40. Rotin, D., and Kumar, S. (2009) Physiological functions of the HECT family of ubiquitin ligases. *Nat. Rev. Mol. Cell. Biol.* **10,** 398–409
41. Macias, M. J., Hyvönen, M., Baraldi, E., Schultz, J., Sudol, M., Saraste, M., and Oschkinat, H. (1996) Structure of the WW domain of a kinase-associated protein complexed with a proline-rich peptide. *Nature* **382,** 646–649
42. Chen, H. I., and Sudol, M. (1995) The WW domain of Yes-associated protein binds a proline-rich ligand that differs from the consensus established for Src homology 3-binding modules. *Proc. Natl. Acad. Sci. U.S.A.* **92,** 7819–7823
43. Nishimura, R., Hata, K., Matsubara, T., Wakabayashi, M., and Yoneda, T. (2012) Regulation of bone and cartilage development by network between BMP signalling and transcription factors. *J. Biochem.* **151,** 247–254
44. Shrivats, A. R., McDermott, M. C., Klimak, M., Averick, S. E., Pan, H., Matyjaszewski, K., Mishina, Y., and Hollinger, J. O. (2015) Nanogel-mediated RNAi against Runx2 and Osx inhibits osteogenic differentiation in constitutively active BMPR1A osteoblasts. *ACS Biomater. Sci. Eng.* **1,** 1139–1150
45. Ali, S. A., Zaidi, S. K., Dobson, J. R., Shakoori, A. R., Lian, J. B., Stein, J. L., van Wijnen, A. J., and Stein, G. S. (2010) Transcriptional corepressor TLE1 functions with Runx2 in epigenetic repression of ribosomal RNA genes. *Proc. Natl. Acad. Sci. U.S.A.* **107,** 4165–4169
46. Gu, G., Nars, M., Hentunen, T. A., Metsikkö, K., and Väänänen, H. K. (2006) Isolated primary osteocytes express functional gap junctions *in vitro*. *Cell Tissue Res.* **323,** 263–271
47. Gan, X. Q., Wang, J. Y., Xi, Y., Wu, Z. L., Li, Y. P., and Li, L. (2008) Nuclear Dvl, c-Jun, β-catenin, and TCF form a complex leading to stabilization of β-catenin-TCF interaction. *J. Cell Biol.* **180,** 1087–1100
48. Gan, X., Wang, J., Wang, C., Sommer, E., Kozasa, T., Srinivasula, S., Alessi, D., Offermanns, S., Simon, M. I., and Wu, D. (2012) PRR5L degradation promotes mTORC2-mediated PKC-δ phosphorylation and cell migration downstream of Gα12. *Nat. Cell Biol.* **14,** 686–696